

---

# Features

---

## MEMS Based Low Power Efficient Capacitive Inverter for renewable energy applications

Ralli Sangno<sup>1,2</sup>, R. K. Mehta<sup>2</sup> and Santanu Maity<sup>3\*</sup>

<sup>1</sup>Dept. of Electrical Engineering, National Institute of Technology, Upia-791112 (e-mail: ralli\_s2001@yahoo.co.in)

<sup>2</sup>North Eastern Regional Institute of Science and Technology, Arunachal Pradesh 791109 (e-mail: rkm@nerist.ac.in)

<sup>3\*</sup>Electronics and Communication engineering, Tezpur University, Tezpur-744028 (e-mail: smaity@tezu.ernet.in)

**Abstract** – In this paper, a micron sized DC/AC power inverter design based on MEMS (micro electromechanical system) is proposed, modeled and demonstrated. The proposed approach uses electrostatic actuation to provide in phase overlap length varying DC/AC inverter system for solar cell application. Two MEMS structures are considered to show good electrical and mechanical performance with zero harmonics and negligible power loss. Also, the actuation voltage is provided under pull in voltage to the actuating part, so that maximum displacement of overlap length is acquired with less instability. The proposed micro scale system exhibits miniaturized volume and expected to acquire improved performance of DC/AC power inverter used for renewable energy applications.

### 1. Introduction

Power inverters are one of the major concerns to be taken care of, in most of the alternative energy systems for the conversion of DC which is obtained from photovoltaic generators into AC. Several researches are going on these days to improve the efficiency of these high rated power inverters [1]. In semiconductor industries, conventional high rated power inverters based on Si power semiconductor device (PSD) are facilitated [2-3]. But, it has several demerits like On-state loss, switching loss of power devices, complex control system configurations, low efficiency, high costs and all these demerits are partially eliminated by PWM Multilevel inverters [4-5]. Even then major challenges are present towards large number of switches to be controlled in multilevel power inverter that causes complexity, presence of harmonics that causes high leakage current and also many more deficiencies strongly affect the DC/AC conversion quality performance. On the other hand, MEMS Inverter approach was proposed as an alternative [6-7]. As the micromachining technology that had emerged in the late 1980s [8]. There are wider application fields of MEMS technology like as, RF-MEMS [9-13], biomedical [14], Aerodynamics [15], thermodynamics [16], telecommunication [17] and so on. It is the well-established technology that provides the low power-actuation, low-cost production and miniaturized volume devices [18-20]. Electrostatic principle is the one that is the most important principle among piezoelectric, electromagnetic and electrostatic principles for the MEMS technology [21].

In this paper, the goal is to demonstrate an implementation of proposed design and mathematical modelling of electromechanical DC/AC inverter system of micron size. The proposed MEMS design is based on comb drive structure for the formation of two sets of variable capacitor (driver and converter). One with two sets of electrodes where one is moving (makes the capacitor variable by to and fro movement) and other is fixed. Moreover, the electrostatic actuation is accomplished by external electrical AC signal to the driving capacitor, thereby enabling variation of overlap length of the converter capacitor for the conversion of solar DC input to AC output. The proposed design is simulated in COMSOL 5.0 to see the resulting mechanical movement of electrodes. On the basis of the design, mathematical expressions are modelled using MATLAB 2013 for suitable desired electrical performance.

### 2. Physical modelling of system design

The design consists of fixed comb electrodes (fixed on anchors), moving comb electrodes, a proof mass (substrate) suspended by double folded flexure (having beams, trusses and anchors) beams and a shuttle mass through which moving comb finger electrodes set attached to the substrate (moving mass) as shown in Figure 1. In this design two capacitive sets formed, exhibit in-phase deflection of overlap lengths when subjected to mechanical movement of moving electrodes

which actually means when the capacitance of one set is increased, the other set of capacitance is also increased. And this deflection makes the capacitors variable in nature where one set of capacitors is working as driving part and other set as converter part of the system.

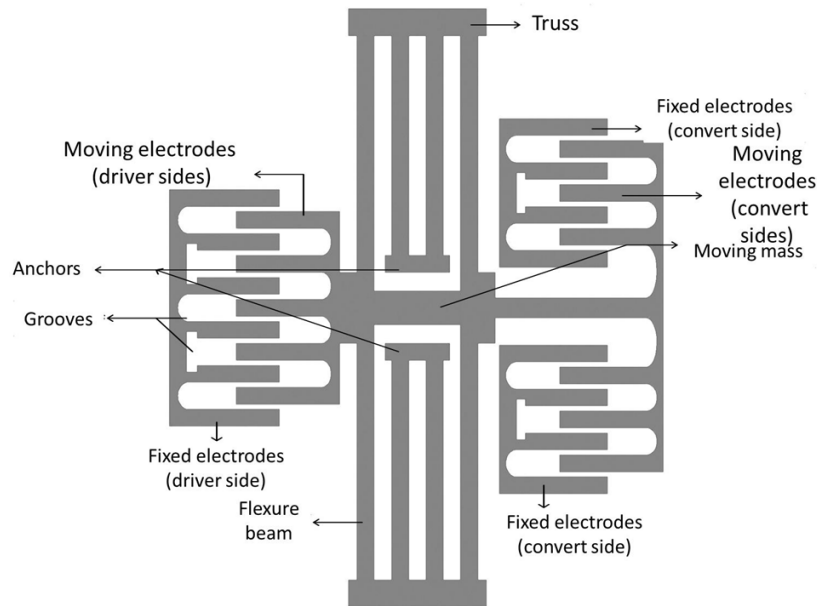


Figure 1: Schematic View of System Design of MEMS Power Inverter.

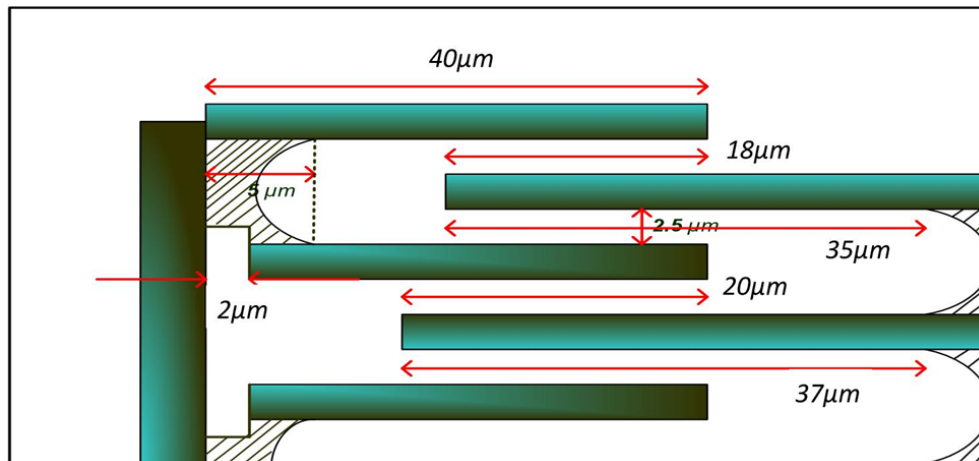


Figure 2: A small part of proposed Interdigitated Capacitor Design (ICD).

The sketch of a small part of the design of comb structure proposed is shown in Figure 2. In the capacitive portion, one moving finger is kept smaller and the next finger of it is kept 1 to 2  $\mu\text{m}$  larger than the previous finger expecting to reduce the fringing effect and to acquire more capacitance formation than the previous work [22]. Also, the proposed design consists of groove shaped structure expecting to reduce the front instability of front part of electrodes as because when the actuation is done, not a single pair of capacitor is formed but more than one capacitance is formed [23]. To lessen the effect of the other pair of capacitors, all these changes in capacitor geometry have been done. Thus sample of the proposed design is implemented by using optimization method (using COMSOL 5.0) in which the comb structure (consisting of moving and fixed limbs) is attached to the double folded flexure [24] spring through the moving mass. The detailed specification of the design and the basic materials used are depicted based on the references [25, 26].

### 3. Operating principle and mathematical representation of MEMS comb structure

The specifications of inputs are provided in Table 1. The equivalent electrical circuit diagram of the proposed system is shown in the Figure 3.

**Table 1** Specifications of the input provided to the system designed

INPUT	VALUES
Reference DC Voltage	23.3 V
Reference AC Perturbed voltage	220 V
Frequency	50- 60 Hz (Range)
Solar DC input	24 V
Load(resistive)	10 K $\Omega$

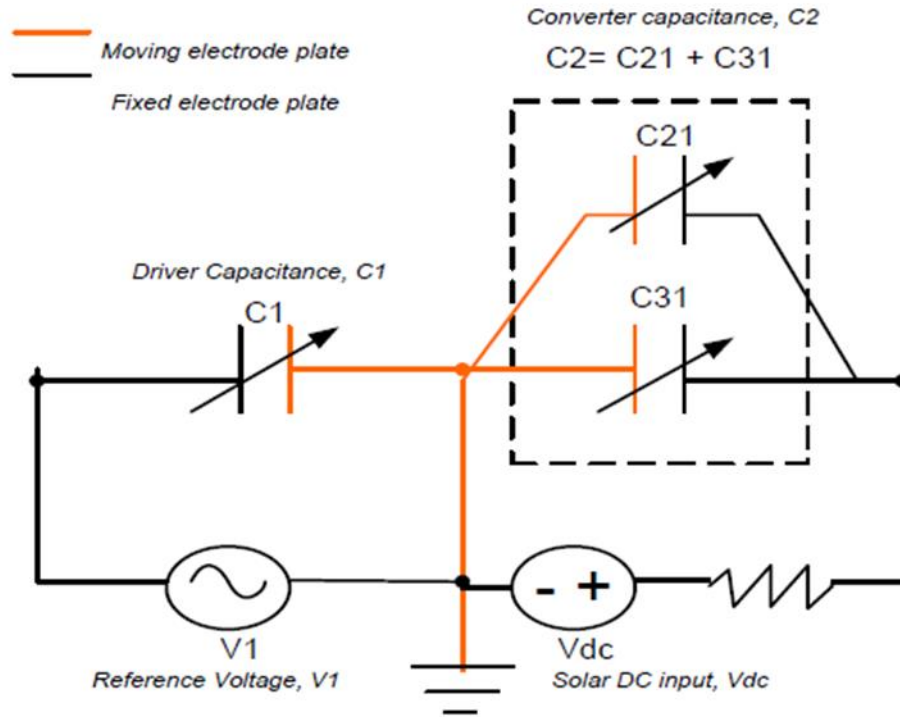


Figure 3: Equivalent Circuit Diagram of MEMS Power Inverter.

Actuating voltage applied on the driving comb structures results in a deflection of the moving fingers in both X and Y directions, but it is preferably in desired Y direction with a small deflection in undesired X-direction because of presence of double folded flexure [22]. The capacitance depends on the geometry of capacitor, not on the applied actuation voltage or accumulated charge. Hence this deflection causes change in overlapping length ( $l_0$ ) and thus the area changes which finally results in variation of capacitance ( $C_{var}(t)$ ) expressed as equation (1).

$$C = \frac{\epsilon_0 \epsilon_r N_e (L_0 + \bar{X}) t_e}{g} \quad (1)$$

where  $\epsilon_0$  = Permittivity of vacuum ( $8.854 \times 10^{-12}$  F/m),  $\epsilon_r$  = Medium dielectric constant (1 for vacuum),  $N_e$  = Number of movable capacitor's electrodes,  $L_0$  = Electrode's initial overlapping length,  $t_e$  = Electrode's thickness,  $g$  = The gap between movable and fixed electrodes. An equal and opposite charges build on the surface of electrodes due to the potential difference between the electrodes (fixed and moving) because of which electrostatic force ( $F_{es}$ ) developed in between the electrodes is

$$F_{es} = \frac{1}{2} \left( \frac{dC_{var}(t)}{dy} \right) V^2 = \frac{1}{2} \left[ \left( \frac{dC_1(t)}{dy} \right) V_1^2 + \left( \frac{dC_2(t)}{dy} \right) V_{2var}^2(t) \right] \quad (2)$$

Where,  $C_1(t)$  =Driving capacitance,  $C_2(t)$  =Equivalent converter capacitance in which the two sets of capacitor are connected in parallel shown in the Figure 4 is

$$C_2(t) = C_{2i} + C_{3j} \quad (3)$$

$i, j=1,2,3,\dots,N_e$

$$\frac{dC_{var}(t)}{dy} = \left\{ \begin{array}{l} \frac{C_0}{I_0}, \bar{y} = y \\ -\frac{C_0}{I_0}, \bar{y} = y \end{array} \right\}, \text{Rate of change of capacitance with displacement}$$

Where  $V_1$  = Driving voltage or reference voltage

$$V_1 = \sqrt{(V_{AC}^2) + (V_{1DC}^2)} \quad (4)$$

Where,  $V_{1DC}$  = Reference DC bias Voltage,  $V_{AC}$  = AC perturbed reference voltage.  $V_1$  can be varied so as to change the amount of charge ( $Q_{c1}$ ) accumulated on the surface of electrodes and moving electrodes allow the use of that charge ( $Q_{c2}(t)$ ) as an intermediate variable which can be used to control the change in  $l_0$  so that  $C_2(t)$  is increased and voltage ( $V_{2var}(t)$ ) across  $C_2(t)$

$$V_{2var}(t) = \frac{1}{C_2(t)} \int i_{var}(t) dt \quad (5)$$

By applying KVL in the electrical domain of converter side, the resulting relation is -

$$V_{2var}(t) = V_{DC} - R_L i_{var}(t) \quad (6)$$

Where  $V_{DC}$  = Solar DC input voltage,  $R_L$  = Load Resistance,  $i_{var}(t)$  = Current in the converter circuit

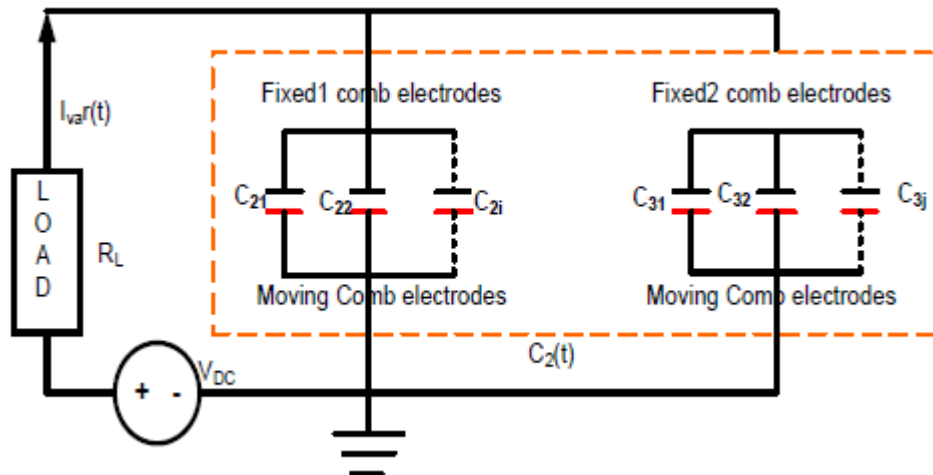


Figure 4: Converter Circuit Diagram in Electrical Domain.

$$i_{var}(t) = \frac{dQ_{c2}(t)}{dt} = \frac{d}{dt} [C_2(t) V_{2var}(t)]$$

$$i_{\text{var}}(t) = V_{2\text{var}}(t) \left[ \frac{dC_2(t)}{dt} \right] + C_2(t) \left[ \frac{dv_{2\text{var}}(t)}{dt} \right]$$

$$V_{DC} - \left\{ \frac{C_2(t)R_L \left[ \frac{di_{\text{var}}(t)}{dt} \right]}{\frac{dC_2(t)}{dt}} \right\} - \left\{ R_L + \frac{1}{\frac{dC_2(t)}{dt}} \right\} i_{\text{var}}(t) = 0$$

$$V_{DC} - L_2(t) \left[ \frac{di_{\text{var}}(t)}{dt} \right] - \{R_L + R_2(t)\} i_{\text{var}}(t) = 0 \quad (7)$$

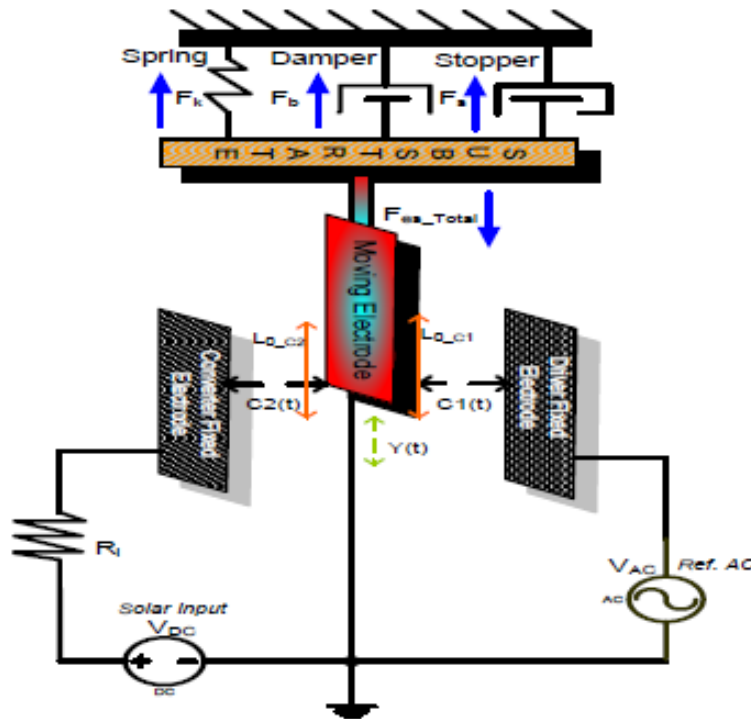


Figure 5: Simplified Circuit Diagram of the proposed MEMS inverter.

The equation (7) represents the converter circuit consists of source  $V_{DC}$  in series with [varying inductor  $L_2(t)$ ] and varying resistor ( $R_2(t)$ ) as new components [18] of  $C_2(t)$  and  $R_L$

$$R_2(t) = \left[ \frac{1}{\frac{dC_2(t)}{dt}} \right] \quad (8)$$

$$L_2(t) = \left[ \frac{R_L C_2(t)}{\frac{dC_2(t)}{dt}} \right] \quad (9)$$

Where, inductive part (9) represents the energy storage element results from coupling between the capacitor converter circuit and the load resistance. Resistive part (8) represents the open circuit resistance meant for the measure of energy dissipation i.e. for minimum internal resistance; we require increment in the value of rate of change of capacitance. Continuously growing of electrostatic force causes the displacement in positive Y-direction. In order to keep the electrodes away from ‘esp of bursting’, an equal and opposite force resisting this motion is modeled by restoring force [27-29] of a mechanical spring with spring constant (k) and a damper with damping coefficient ( $b_m$ ). The total force acting on the system design is shown in the Figure 5.

The balance force is defined as equation 10.

$$my + b_m y + ky + F_s = mA_{es} + F_{es} \quad (10)$$

The term, mechanical stopper force ( $F_s$ ) is the resultant mechanical force used to limit the deflection of moving mass by

$$F_s = \begin{cases} 0, & -y_s \leq y \leq y_s \\ k_s(y+y_s), & y < -y_s \\ k_s(y-y_s), & y > y_s \end{cases}$$

Where,  $k_s$  =Stiffness constant of stopper  $\pm y_s$  = Moving mass deflection limit.

#### 4. Results and discussion

Mathematical modeling of the proposed MEMS power inverter is simulated using MATLAB Simulink to determine the resulting plots of converted AC voltage and force versus displacement shown in the Fig 6. It is observed from the plots that converted AC voltage obtained is of amplitude 4.7V across the Load (10 K $\Omega$ ) at the solar input of 19.6V when the system is being actuated by reference of 130V, 50 Hz; AC and 3V; DC bias voltage for 2 seconds. The electrostatic force built up to  $16.6 \times 10^{-4}$  N which facilitates the maximum displacement of overlap length up to 9  $\mu$ m.

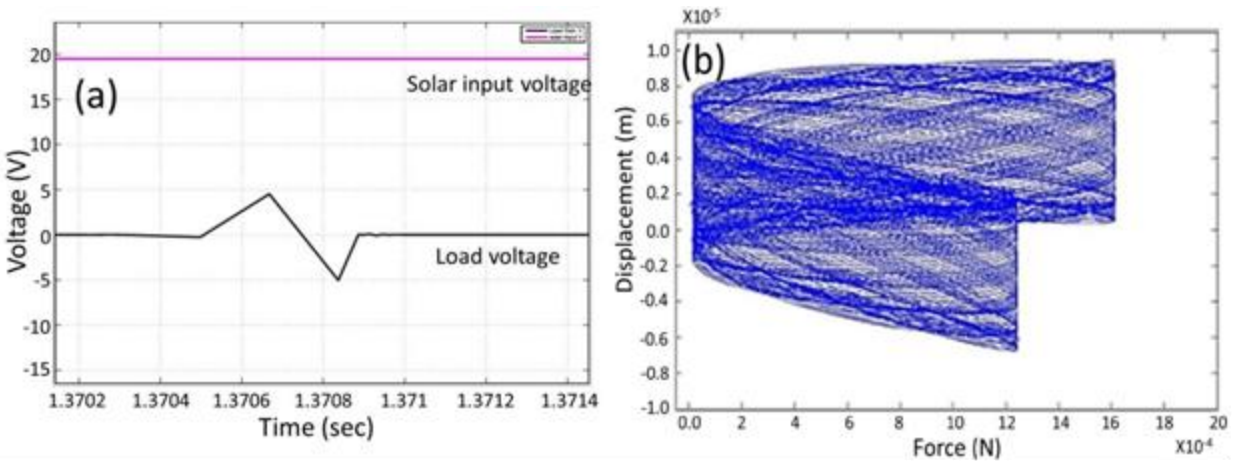


Figure 6: Converted Voltage across Load with Solar Input Voltage Versus time Plot, (b) Force Built up Versus Displacement Plot

For the concept demonstration and the comparison purposes, only a half part of the proposed design is simulated in COMSOL 5.0 Multiphysics taking two cases (a) simple rectangular and (b) modified rectangular grooved comb drive structure. Comparisons of two different cases (models) are done on the basis of the following parameters like electric potential distribution, displacement and capacitance variation. The resulting surface plot of electric potential distribution and the displacement facilitated by actuation voltage of 23.3V for both the models. Also, the displacement and capacitance variation with respect to the applied voltage can be seen and measured clearly from Fig.7.

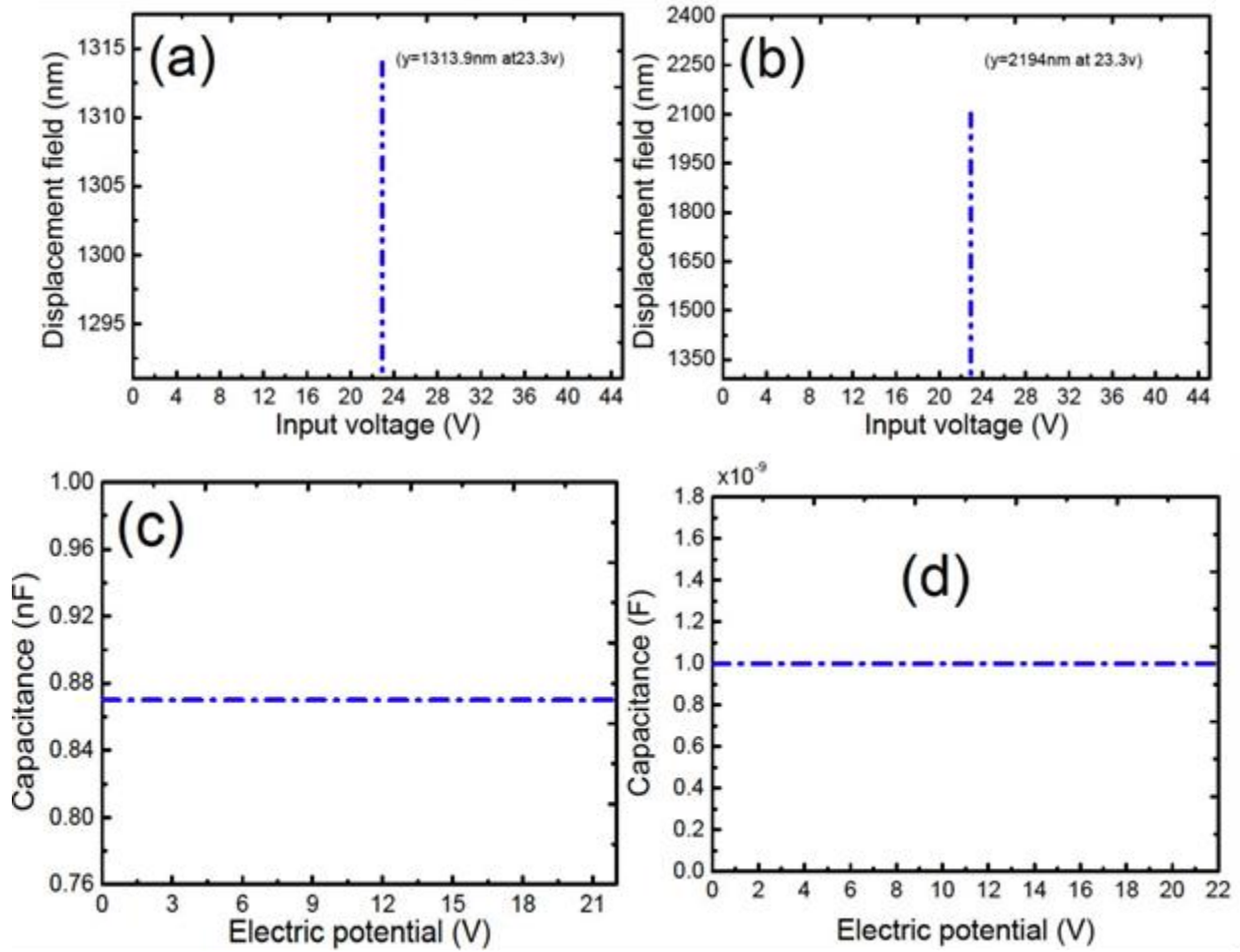


Figure 7: (a), (b) Displacement(y) Vs applied Voltage for both the models (1 & 2), (c)(d) Capacitance(C) Vs. Electric Potential for both the models (1 & 2) ( $C=0.8701\text{nF}$   $C=0.9623\text{n}$ )

**Table 2 Resulting Values of Plot 7**

DESCRIPTION	INPUT	MAXIMUM	CAPACITANCE
	VOLTAGE	DISPLACEMENT	VALUE
<b>Model 1</b>	23.3 V	(1289.7-1313.9) nm	0.8701 nF
<b>Model 2</b>	23.3 V	(2189.6-2194) nm	0.9623 nF

It is seen in figure 7 that the displacement and capacitance values of case I are more than case 2 (table 2). Actuation depends on the number of comb fingers [24] which is related to electrostatic force and capacitance. Surface electric potential and displacement plot of the moving electrodes are observed so that the capacitance formed due to the fixed and moving electrodes are being varied and the graphs are obtained and shown in the figure 8. Displacement shown in the fig. 8 (b) is towards the Y-direction that actually meant for the enhancement of the overlap length of the capacitors because of which the overlapping area increases. The increase in overlapping area facilitates the increase of capacitance across the converter circuit.

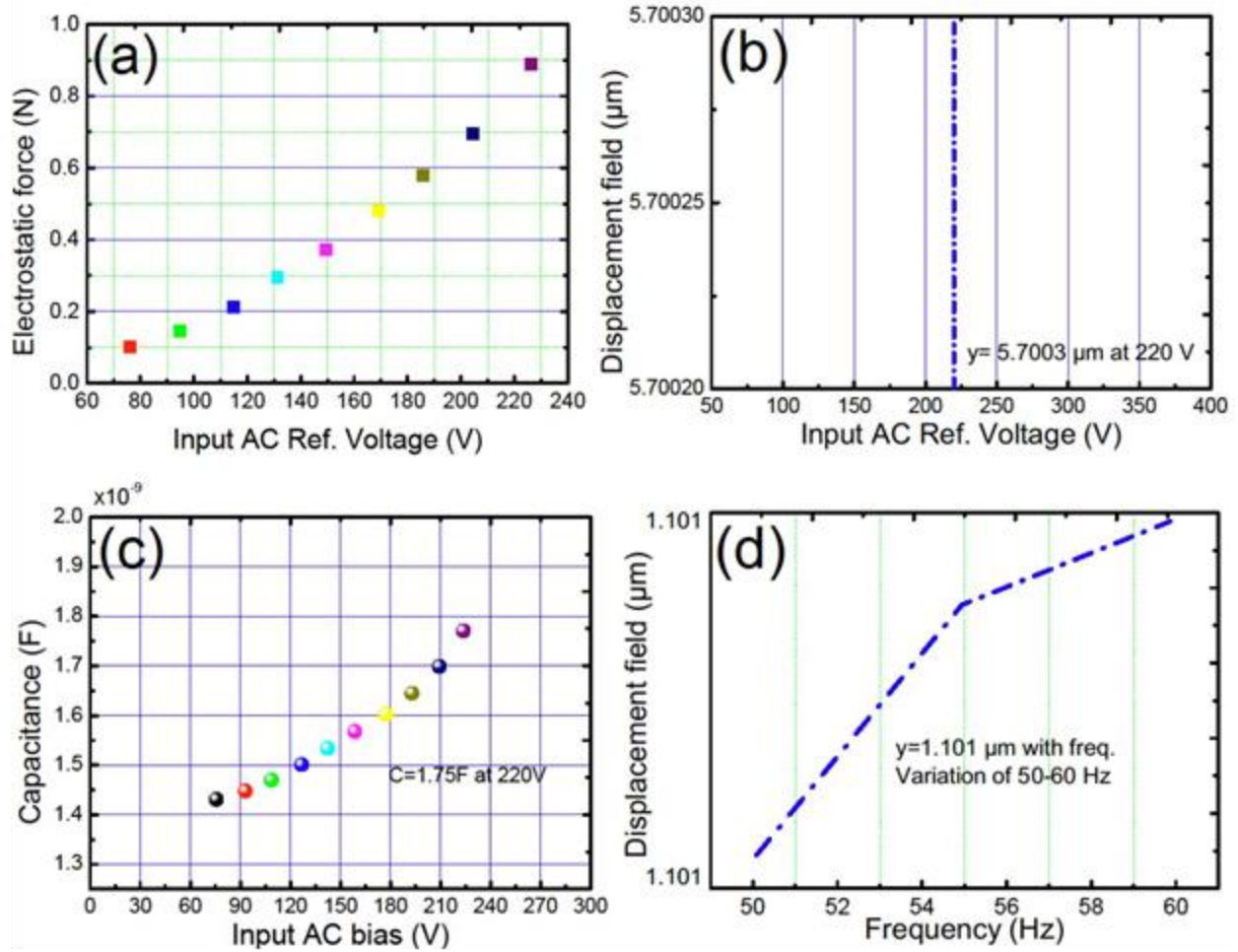


Figure 8: (a) Electrostatic force (F) Vs Reference Voltage ( $F = 0.84 \text{ N}$  at  $220 \text{ V}$ ), (b) Displacement ( $y$ ) Vs Actuation Voltage (V), (c) Capacitance (C) Vs Actuation Voltage, (d) Displacement ( $y$ ) versus Frequency ( $f$ ) (Hz).

From the plots in Figure 8, it is seen that due to the actuation voltage, the electrostatic force is built up in between the two electrodes (fixed and moving) which is proportional to the square of the applied voltage and its variation with different values of voltage is shown by the plot 8(a). The electrostatic force further causes the displacement in overlap length which then induces change in capacitance and as the capacitance is inversely proportional to the voltage; here its variation with voltage is shown in Fig. 8(c). Also, the displacement depends on the frequency of the AC perturbed reference voltage which can be clearly shown by the plot (d) of Figure 8. Low power VLSI application is major concert in the current technology [30, 31]. The proposed model is applicable for low cost and low power application.

## 5. Conclusion

This paper proposed a solution to the critical problem of DC/AC conversion quality performance of commercial power inverter used for renewable energy applications by adopting the MEMS based capacitive power inverter system. Owing to the proposed concept, mechanical part of the system is designed to have a high level of stiffness in order to be actuated by the power grid voltage. The proposed MEMS approach enables the non-complexity of the inverter, zero harmonics, miniaturized volume device, low cost production and very less losses (almost lossless). It also doesn't consume power for the DC/AC conversion process. It is developed in this work by means of simulations of two models for comparison and the modified comb drive design is proposed so as to lessen the instabilities with acquisition of more capacitance formation across interdigitated electrodes so that it can be directly used in MEMS capacitive Transducer.

**Acknowledgement:** The respective work was supported by Jadavpur University so that the design is simulated in COMSOL 5.0 to see the resulting movement of mechanical part of the system after being actuated electrically.

## Reference

- [1] A. Ravindranath; O. Ray; S. Mishra; A Joshi, “Single phase utility interactive switched Boost Inverter for Renewable Energy based residential power applications” APEC 2013, Twenty Eighth Annual IEEE Year:2013, pages :3283-3287, DOI :10.1109/APEC.2013.6520771
- [2] A. Aganza-Torres; V. Cardenas , “Analysis and Modelling of HF Link Cycloconverter based inverter for low-power Renewable Energy Sources application”; CCE, 2011, Seventh International Conferences on the Year: 2011, pages: 1-6, DOI: 10.1109/CEEE.2011.6106602
- [3] B.R. Lin; J.J Chen, Three-Phase Two-Leg inverter for stand-alone and grid- connected Renewable Energy systems” TENCON 2006. 2006 IEEE Region 10 Conferences Year: 2006, pages: 1-4, DOI: 10.1109/TENCON.2006.344163
- [4] K. Hirrachi, M. Ishitobi, K. Matsumoto, H. Hattori, M. Ishibashi, M. Nakaoka, N. Takahashi, Y. Kato; Pulse Area Modulation control implementation for single phase current source –fed inverter for solar photovoltaic power conditioner” Volume-2, pages: 677-682 Vol.2, DOI: 10.1109/PEDES.1998.133068
- [5] D.M. Reddy, T. Gowrimanohar; “Dynamic Performance of Power quality improvement using Multilevel DSTATCOM with DG applications” ICCTET, 2014, Second International Conference on the Year: 2014, pages: 288 - 295; DOI – 10.1109/ICCTET.2014.6966304
- [6] Shuo Cheng And David P. Arnold , “A resonant DC/AC Inverter using an electromechanical device”, pages: 1-4; on the year 2011
- [7] Subha Chakraborty, T.K. Bhattacharyya; “Development of a Micro-Mechanical Logic Inverter for Low Frequency MEMS Sensor Interfacing” 2011, 24th Annual Conference on VLSI Design; IEEE, DOI 10.1109/VLSID.2011.26
- [8] Prime Faraday Partnership, “An introduction to MEMS (Micro - electromechanical System)” Wolfson School of Mechanical and Manufacturing Engineering Loughborough University; 2002, ISBN 1-84402-020-7
- [9] Rajesh Saha, Santanu Maity, Chandan Tilak Bhunia, Design and Characterization of a Tunable Patch Antenna Loaded with Capacitive MEMS Switch using CSRRs Structure on the Patch", Alexandria Engineering Journal, Elsevier, Volume 55, Issue 3, Pages-2621–2630, (2016),
- [10] Anwesha Choudhury, Santanu Maity, Design and fabrication of CSRR based tunable mechanically and electrically efficient band pass filter for K-band application, AEU - International Journal of Electronics and Communications, Volume 72, February 2017, Pages 134-148
- [11] Rajesh Saha, Santanu Maity, Ngasepam Monica Devi, Chandan Tilak Bhunia, Analysis of Pull-in-Voltage and Figure-of-Merit of Capacitive MEMS switch, Transactions on Electrical and Electronic Materials , April, 2016, Volume 17 Number 3, June 25, 2016,
- [12] Rajesh Saha, Santanu Maity, Ngasepam Monica Devi, Chandan Tilak Bhunia, Analysis of Pull-in-Voltage and Figure-of-Merit of Capacitive MEMS switch, Transactions on Electrical and Electronic Materials , April, 2016, Volume 17 Number 3, June 25, 2016,
- [13] Avra Kundu, Sonali Das, Santanu Maity, Bhaskar Gupta, Samir K Lahiri and Hiranmay Saha “A tunable band-stop filter using a metamaterial structure and MEMS bridges on a silicon substrate” (JOURNAL Micromech. Microeng. 22 (2012 (IOP)) 045004 (12pp))
- [14] “MEMS technology for biomedical applications” D.L. Polla IEEE, Year-2001 Page(s):19-22 vol. 1, DOI: 10.1109/CSICT.2001.981417
- [15] H. Babinsky, U. Kuschel, H.P. Hodson, D.F. Moore and M.E. Welland “The Aerodynamic Design and Use of Multi-sensor Pressure Probes for MEMS Applications” Year-2000 Page(s):1-7
- [16] R.W. Whatmore, “Uncooled pyroelectric detector arrays using ferroelectric ceramics and thin films” MEMS Sensor Technologies, 2005 IET Conference, Year-2005 Page(s):11, DOI:10.1049/ic:20050116
- [17] D. Dellaert, J. Doutreloigne, “Latching MEMS switch matrices for telecommunication applications” 2015 16th International Conference, Year-2015 Page(s):1-6, DOI:10.1109/EuroSimE.2015.7103079
- [18] S.S. Je, F. Rivas, R.E. Diaz, J. Kwon, J. Kim, B. Bakkaloglu, S. Kiaei, J. Chae; “A compact and Low-cost MEMS loudspeaker for Digital Hearing Aids” IEEE transactions on Biomedical Circuits and Systems Year-2009, volume:3, Page(s):348-358, DOI:10.1109/TBCAS.2009.2026429

- [19] Hussam A. Kloub , Eyad M. Hamad, “Electromechanical modeling and designing of capacitive MEMS DC/AC interactive power inverter for Renewable Energy Applications”, *Microsyst Technol*; Technical Paper, 9 December 2015, DOI 10.1007/s00542-015-2767-1
- [20] Min-Wu Kim, Yong-Ha Song, Hyun-Ho Yang and Jun-Bo Yoon, “An ultra-low voltage MEMS switch using stiction-recovery actuation” 2013 *Journal of Micromechanics and Microengineering*, Year-2013 Page(s)-1-8, DOI:10.1088/0960-1317/23/4/045022
- [21] Joydeep Basu and Tarun Kanti Bhattacharyya, “Microelectromechanical Resonator for Radio Frequency Communication Applications” Oct 2011, Vol. 17(10-11), pp. 1557-1580 Springer-Verlag 2011, DOI:10.1007/s00542-011-1332-9
- [22] Shefali Gupta, Tanu Pahwa, Rakesh Narwal, B.Prasad, Dinesh Kumar, “Optimizing the Performance of MEMS Electrostatic Comb Drive Actuator with Different Flexure Springs”, *Electronic Science Department, Kurukshetra University, Kurukshetra, Haryana, 2012*
- [23] Hussam Abdel Hamid Kloub, “High Effectiveness Micro Electromechanical Capacitive Transducer for Kinetic Energy Harvesting” October 2011, Disputation Year-8th Feb 2012, IMTEK
- [24] Venkatesh.M, Krushnasamy.V.S, “Design and Analysis of Double folded Beam MEMS accelerometer”, *International Journal of Advanced Research in Electrical and Electronics and Instrumentation Engineering*, vol.3, March 2014 page(s): 1-6
- [25] Swati Kapoor, Dinesh Kumar, B.Prasad, Anil Gujjar, Vineet Bansa “MEMS Electrostatic comb actuators with different configurations: A comparison of structure design and materials using COMSOL 3.5a, , 2011 COMSOL Conference in Bangalore, Electronics Science Department, Kurukshetra University, Year- 2011, page(s):1-5
- [26]”, Lars Geir Whist Tvedt, Lars-Cyril Julin Blystad and Einar Halvorsen, “Simulation of an Electrostatic Energy Harvester at Large Amplitude Narrow and Wide Band Vibrations 9-11 April 2008, DTIP 2008 ISBN: 978-2-35500-006-5, Year-2008 Page(s):1-6
- [27] M. Sterner, N. Roxhed, G. Stemme, J. Oberhammer; “Mechanically tri-stable SPDT metal-contact MEMS switch embedded in 3-D transmission line” *Microwave Integrated Circuit Conference, 2007; EuMIC 2007. European*, Year-2007 Page(s):427-430, DOI:10.1109/EMICC.2007.4412740
- [28] Dong- ha Shim, Seoul (KR); “MEMS device having flexures with Non- Linear restoring force”, U.S. patent 6,806,545 B2; 19 Oct. 2004, page(s): 1-9
- [29] R Sangno, RK Mehta, S Maity, Improvement in capacitive performances of efficient micro electro mechanical system (MEMS) based power inverter, *Cogent Engineering* 4, 1455407, 2018
- [30] Krishna Prasad Gnawali, Seyed Nima Mozaffari, Low Power Artificial Neural Network Architecture, *IEEE VLSI Circuits and Systems Letter*, Volume 4, Issue 4, Nov 2018
- [31] Priyank Sharma and Sanjay Sharma, Evaluation of Ultra-Low Power Techniques to 10T Junction Less Double Gate Hybrid Full Adder (10TJLDGFHA), *IEEE VLSI Circuits and Systems Letter*, Volume 4, Issue 4, Nov 2018

## About the Authors

---